Cancer Science
Japanese Cancer Association JCA
Open Access

# Calreticulin is highly expressed in pancreatic cancer stem-like cells

Satoshi Matsukuma,[1] Kiyoshi Yoshimura,[1,2] Tomio Ueno,[1] Atsunori Oga,[3] Moeko Inoue,[1,2] Yusaku Watanabe,[1] Atsuo Kuramasu,[4] Masanori Fuse,[2] Ryouichi Tsunedomi,[1] Satoshi Nagaoka,[5] Hidetoshi Eguchi,[5] Hiroto Matsui,[1] Yoshitaro Shindo,[1] Noriko Maeda,[1] Yoshihiro Tokuhisa,[1] Reo Kawano,[6] Tomoko Furuya-Kondo,[3] Hiroshi Itoh,[3] Shigefumi Yoshino,[1,7] Shoichi Hazama,[1,8] Masaaki Oka[1] and Hiroaki Nagano[1]

[1]Department of Gastroenterological, Breast and Endocrine Surgery, Yamaguchi University Graduate School of Medicine, Ube; [2]Exploratory Oncology Research and Clinical Trial Center, National Cancer Center of Japan, Tokyo; Departments of [3]Molecular Pathology; [4]Molecular Pharmacology, Yamaguchi University Graduate School of Medicine, Ube; [5]Gastroenterological Surgery, Osaka University Graduate School of Medicine, Suita; [6]Center for Clinical Research; [7]Oncology Center, Yamaguchi University Hospital, Ube; [8]Department of Translational Research and Developmental Therapeutics against Cancer, Yamaguchi University Graduate School of Medicine, Ube, Japan

**Key words**

Biomarkers, calreticulin, cancer stem cells, pancreatic cancer, proteomics

**Correspondence**

Kiyoshi Yoshimura, Exploratory Oncology Research and Clinical Trial Center, National Cancer Center of Japan, 5-1-1 Tsukiji, Chuo-ku, Tokyo 104-0045, Japan.
Tel: +81-3-3547-5201; Fax: +81-3-3543-6283;
E-mail: kiyoshim@ncc.go.jp

**Funding Information**

Yamaguchi University Hospital.

Received May 14, 2016; Revised August 5, 2016; Accepted August 14, 2016

*Cancer Sci* **107** (2016) 1599–1609

doi: 10.1111/cas.13061

**Cancer stem-like cells (CSLCs) in solid tumors are thought to be resistant to conventional chemotherapy or molecular targeting therapy and to contribute to cancer recurrence and metastasis. In this study, we aimed to identify a biomarker of pancreatic CSLCs (P-CSLCs). A P-CSLC-enriched population was generated from pancreatic cancer cell lines using our previously reported method and its protein expression profile was compared with that of parental cells by 2-D electrophoresis and tandem mass spectrometry. The results indicated that a chaperone protein calreticulin (CRT) was significantly upregulated in P-CSLCs compared to parental cells. Flow cytometry analysis indicated that CRT was mostly localized to the surface of P-CSLCs and did not correlate with the levels of CD44v9, another P-CSLC biomarker. Furthermore, the side population in the $CRT^{high}/CD44v9^{low}$ population was much higher than that in the $CRT^{low}/CD44v9^{high}$ population. Calreticulin expression was also assessed by immunohistochemistry in pancreatic cancer tissues ($n = 80$) obtained after radical resection and was found to be associated with patients' clinicopathological features and disease outcomes in the Cox proportional hazard regression model. Multivariate analysis identified CRT as an independent prognostic factor for pancreatic cancer patients, along with age and postoperative therapy. Our results suggest that CRT can serve as a biomarker of P-CSLCs and a prognostic factor associated with poorer survival of pancreatic cancer patients. This novel biomarker can be considered as a therapeutic target for cancer immunotherapy.**

Pancreatic cancer is an aggressive type of malignancy and the fifth leading cause of cancer-related death in Japan (Center for Cancer Control and Information Services, National Cancer Center, Japan). Most patients present with locally advanced disease or systemic metastasis at diagnosis, and only 15–20% of them have resectable tumors.[1] Major hallmarks of this cancer are the resistance to conventional chemotherapy and radiation therapy, and a high relapse rate after radical surgery.

Emerging evidence suggests that the low sensitivity of pancreatic tumors to conventional treatment, and, consequently, high rate of local recurrence and distant metastasis may be attributed to a small subset of cells known as CSLCs.[2–4] Therefore, to increase the efficiency of pancreatic cancer therapy and improve the disease outcome, it is critically important to determine the biological properties of CSLCs and to develop CSLC-targeting strategies.

It has been reported that the tumorigenic subpopulation of pancreatic cancer cells is characterized with high expression of CD44, CD24, and epithelial-specific antigen.[5] Moreover, CD133,[6] aldehyde dehydrogenase 1,[7] c-Met,[8] and doublecortin-like kinase 1[9] have been established as major biomarkers of pancreatic CSLCs. A recent study has shown that in gastrointestinal cancer cells, elevated expression of CD44, especially its variant isoforms (CD44v), is associated with increased defense against ROS through upregulation of reduced glutathione synthesis, which contributes to cancer cell survival and drug resistance.[10]

We have developed a novel technique to generate P-CSLC-enriched populations with increased expression of CD44 and CD24 ($CD24^{high}/CD44^{high}$) from pancreatic cancer cell lines in serum-free medium.[11] Moreover, these $CD24^{high}/CD44^{high}$ cells are also characterized with higher levels of CD44v compared to parental cells.

Although a number of P-CSLC molecular markers have been described, few clinical trials targeting P-CSLCs have been undertaken (ClinicalTrials.gov identifier: NCT01088815), indicating the need of identifying novel P-CSLC-specific molecules such as CD44v,[10,12] and elucidating their role in the pathophysiology of pancreatic cancer.

Calreticulin is a 46–65-kDa chaperone protein located in the ER that has diverse roles in cellular metabolism, including $Ca^{2+}$ homeostasis, cell adhesion, and HLA class I assembly. Recent studies indicate that chemotherapeutic agents such as mitoxantrone and oxaliplatin trigger CRT translocation from

the ER to the cell surface, resulting in induced anticancer immune response;[13,14] it has also been suggested that anti-CRT antibodies can be used for the early diagnosis of pancreatic cancer.[15] However, CRT overexpression has been associated with the development and progression of pancreatic cancer.[16] Although the role of CRT in cancer is still controversial, these data indicate that the surface expression of CRT induces overwhelming anticancer immune response and may confer an aggressive phenotype to pancreatic cancer cells.

In this study, we found, using our method of P-CSLC induction and a proteomics-based approach, that CRT and CD44v9 were upregulated in P-CSLCs and that increased CRT expression was associated with poorer survival of pancreatic cancer patients.

## Materials and Methods

**Cell lines and culture conditions.** Human pancreatic cancer cell lines YPK2 and YPK5 were established in our department.[17] Human colorectal adenocarcinoma cell line SW480 was purchased from ATCC (Manassas, VA, USA) within 6 months before the experiment. The cells were maintained in DMEM-F12 (Sigma-Aldrich Japan, Tokyo, Japan) supplemented with 10% heat-inactivated FBS (Life Technologies, Tokyo, Japan) at 37°C in 5% $CO_2$.

**Induction of P-CSLCs.** Cancer stem-like cell-enriched populations were obtained from YPK and SW480 cells as previously described.[11] In brief, cells were first cultured in serum-free medium containing LIF (Merck Millipore, Darmstadt, Germany), NSF-1 (Lonza, Tokyo, Japan), and NAC (Sigma-Aldrich Japan) to induce tumor spheres. The obtained spheres were collected and transferred to laminin-coated dishes with sphere culture medium containing B27 supplement (Life Technologies), epidermal growth factor (Sigma-Aldrich Japan), and basic fibroblast growth factor (Merck Millipore); half of the medium was changed every week. The resultant cells, designated YPK2-Lm, YPK5-Lm, and SW480-Lm, gradually attached to the substratum and grew for 1–2 months; they were used to identify molecules differentially expressed in P-CSLCs and parental cells by proteomics.

**Sample preparation and 2-D electrophoresis.** Dead cells were eliminated from the cultures by labeling with Dead Cell Removal MicroBeads (Miltenyi Biotec, Gladbach, Germany) and separation in an LS column using magnetic field generated by a MidiMACS Separator (Miltenyi Biotec). CD44v9-positive cells were selected using anti-CD44v9 rat IgG (clone RV3; Cosmo Bio, Tokyo, Japan), biotin-conjugated anti-rat mouse IgG (eBioscience, San Diego, CA, USA) and microbeads carrying anti-biotin mouse IgG (Miltenyi Biotec), and isolated using the MidiMACS Separator.

For protein extraction, YPK parental cells and YPK-Lm-derived CD44v9-positive cells were washed twice with PBS, centrifuged, and stored at −20°C until use. Each sample was suspended in 0.2% Pharmalyte and homogenized in 0.34 mL lysis buffer containing 5 M urea, 2 M thiourea, 2% (w/v) CHAPS, 2% (w/v) SB3-10, 1% (w/v) DTT (all reagents from Sigma-Aldrich Japan). The protein concentration in each sample was measured using a protein assay kit (Bio-Rad, Hercules, CA, USA), and 2-D electrophoresis was carried out as previously described.[18]

Briefly, the samples were applied to 18-cm Immobiline DryStrips (pH 3–10; GE Healthcare, Tokyo, Japan) overnight and subjected to isoelectric focusing using CoolPhoreStar IPG-IEF Type-P (Anatech, Tokyo, Japan) under the following conditions: 500 V for 1 min and 3500 V for 7.5 h at 20°C. After equilibration in 50 mM Tris–HCl (pH 6.8), 6 M urea, 32% glycerol, 10% SDS, and 0.25% DTT followed by 50 mM Tris–HCl (pH 6.8), 6 M urea, 32% glycerol, 10% SDS, 4.5% iodoacetamide, and 0.125% bromophenol blue, the DryStrips were subjected to second-dimension gradient electrophoresis (9–18% acrylamide; Towa Environment Science, Osaka, Japan) using an Anderson ISO-DALT Multiple Electrophoresis System (Hoefer, Holliston, MA, USA) at 80 V for 16 h; broad-range molecular weight markers (V8491) were obtained from Promega (Tokyo, Japan). After staining with SYPRO Ruby protein gel stain (S21900; Thermo Fisher Scientific, Waltham, MA, USA), protein spots were detected using a Molecular Imager FX (Bio-Rad, Tokyo, Japan) and analyzed with ImageMaster 2D Platinum software (GE Healthcare). Common protein spots with higher intensity in both YPK2-Lm and YPK5-Lm compared to respective parental cells were excised and subjected to further analysis.

**Matrix-assisted laser desorption/ionization time of flight mass spectrometry and tandem mass spectrometry.** The excised samples were destained in 15 mM potassium ferricyanide and 50 mM sodium thiosulfate (Wako, Osaka, Japan), washed in 100 mM $NH_4HCO_3$ (Sigma-Aldrich, St. Louis, MO, USA) with agitation for 20 min, and dehydrated with acetonitrile (Wako) in a vacuum centrifuge. The gels were rehydrated in digestion solution containing 50 mM $NH_4HCO_3$, 5 mM $CaCl_2$, and 0.01 μg/μL trypsin (Promega, Madison, WI, USA) at 37°C for 16 h; digestion was terminated with 5% TFA. Peptides were extracted with 5% TFA in 50% acetonitrile for 20 min three times, and the combined extract was concentrated to 10 μL in a vacuum centrifuge.

The samples were absorbed to ZipTip C18 pipette tips (ZTC18S960; Merck Millipore) and the peptides were eluted with 0.1% TFA in 50% acetonitrile. A 1-μL aliquot of the eluted sample was mixed with an equal volume of matrix solution (0.3 g/L α-cyano-4-hydroxycinnamic acid, 33% acetone, and 66% ethanol; all from Wako), placed onto a target plate (MTP Anchorchip 600/384; Bruker Daltonics, Bremen, Germany), dehydrated, and analyzed using a mass spectrometer (Ultraflex TOF/TOF; Bruker Daltonics) operated in positive ion reflector mode (20–4000 m/z).

The obtained MS/MS spectra were searched against the NCBInr database using the Mascot database search engine (Matrix Science, London, UK) based on the following parameters: (i) species, mammals; (ii) enzyme, trypsin; (iii) fixed modification, carbamidomethylation; (iv) variable modification, methionine oxidation; (v) peptide tolerance, ±0.1 Da; (vi) MS/MS tolerance, ±0.8 Da; and (vii) missed cleavages, 1.

**Flow cytometry.** The correlation between CRT and CD44v9 expression in YPK2-Lm and YPK5-Lm cells was analyzed by flow cytometry (the protocol is described in Data S1). We also examined whether the surface expression of CRT correlated with that of CD47 (antiphagocytic signal) according to a previously reported procedure.[19]

**Cell sorting.** Cell suspensions were incubated with rat anti-CD44v9 (clone RV3; Cosmo Bio) and rabbit Alexa Fluor 647-conjugated anti-CRT (clone EPR3924; Abcam, Cambridge, MA, USA) for 30 min at 4°C. The binding of anti-CD44v9 antibodies was detected using FITC-conjugated mouse anti-rat IgG (eBioscience) for 30 min at 4°C. $CRT^{high}/CD44v9^{low}$, $CRT^{low}/CD44v9^{high}$, and $CRT^{high}/CD44v9^{high}$ populations were sorted by BD FACSAriaII (BD Biosciences, San Jose, CA, USA). These sorted cells were used in the following analysis of ABC transporter activity.

**Analysis of ABC transporter activity in YPK-Lm cells.** Increased functional activity of ABC transporters is characteristic for drug-resistant cancer cells.[20] It has been shown that an SP of murine hematopoietic stem cells in bone marrow can efflux Hoechst 33342 dye,[21] suggesting activation of ABC transporters. To analyze ABC transporter activity, YPK2-Lm and YPK5-Lm and their corresponding parental cells were suspended in 5% FBS-containing DMEM at the concentration of $1 \times 10^6$ cells/mL, and incubated with 5 μg/mL Hoechst 33342 (Sigma-Aldrich Japan) at 37°C for 30 min. After washing, cells were resuspended in 2% FBS-containing PBS at the concentration of $1 \times 10^7$ cells/mL, and examined using a BD LSRFortessa X-20 cell analyzer (BD Biosciences). Hoechst was excited with a 375-nm trigon violet laser, and dual fluorescence signals were detected using 450/20 (Hoechst 33342-Blue) and 670 LP (Hoechst 33342-Red) filters.

**Patients and tissue samples.** This retrospective study included patients who were diagnosed with invasive ductal carcinoma according to the Japan Pancreas Society classification[22] and underwent radical resection with D2 or more lymph node dissection at Yamaguchi University Hospital (Ube, Japan) between June 2001 and June 2013, and in Osaka University Hospital (Suita, Japan) between March 2007 and October 2012. Patients who died of surgery-related causes and those with other cancers, serous and mucinous cystic neoplasms in the pancreas, pancreatic cancers derived from intraductal papillary-mucinous neoplasms, and pathologically positive or indeterminate margins were excluded. Resected specimens without residual cancer were also not considered.

The information about patients' clinicopathological characteristics was obtained from medical records. This study was approved by the institutional review boards of Yamaguchi University Hospital and Osaka University Hospital (protocol number H27-007). Informed consent was waived because this was a historical cohort study.

**Immunohistochemistry.** Resected tumor samples were analyzed by IHC (protocol is described in Data S1). Immunostained tissue sections were reviewed and scored independently by two authors (A.O. and T.F.) with expertise in pancreatic pathology, who were blind to patients' background. We used a previously described scoring method[23] with minor modification. Briefly, the staining intensity of tumor cells was scored as: (i) absent or weak, 1 point; (ii) moderate, 2 points; and (iii) strong, 3 points. Each intensity was calculated by multiplying the intensity score by the percentage of positive tumor cells and then summing the values to obtain the final IHC score.

**Immunofluorescence staining.** After sample deparaffinization, rehydration, and antigen retrieval by heating in citrate buffer (10 mM, pH 6.0) for 10 min at 95°C, 4-μm tissue sections were cut and blocked in PBS containing 5% normal goat serum and 0.3% Triton X-100 for 60 min at room temperature. Slides were then incubated with an anti-CRT antibody (1:200 dilution; FMC75, Abcam) for 1 h and Alexa Fluor 488-conjugated anti-mouse IgG (1:1000 dilution; #4408, Cell Signaling Technology, Denver, MA, USA) for 1.5 h, followed by anti-CD44v9 rat antibody (1:100 dilution; RV3, Cosmo Bio) for 1 h and Alexa Fluor 555-conjugated anti-rat IgG (1:1000 dilution; #4417, Cell Signaling Technology) for 1.5 h. After washing, sections were overlaid with DAPI-containing ProLong Gold Antifade Reagent (#8961; Cell Signaling Technology) and examined under a phase-contrast microscope (BZ-X700; Keyence, Osaka, Japan). The brightness/contrast adjustment was applied to the whole image.

**Statistical analysis.** Data are presented as the means ± SD, and the difference between samples was analyzed by Student's *t*-test or the $\chi^2$-test. The Kaplan–Meier method was used to calculate recurrence-free and overall survival, and differences were evaluated by the generalized Wilcoxon test. Independent prognostic factors for overall survival were analyzed with Cox's proportional hazard regression model in a stepwise manner. Statistical analyses were carried out using Statflex version 6 (Artec, Osaka, Japan), and $P < 0.05$ was considered significant.

## Results

**Identification of CRT.** A flow chart of our study is shown in Figure S1. First, we compared protein expression in YPK-Lm and respective parental cells by 2-D electrophoresis. A protein spot with the expression 4.43-fold and 5.80-fold higher in YPK2-Lm and YPK5-Lm cells, respectively, compared to the corresponding parental cells, was detected (Fig. 1a–d, arrow) and identified by MALDI TOF/TOF MS as CRT (NCBI accession no. gi|4757900) (Fig. 1e). As the role of CRT in CSLCs is unclear, we undertook further analysis of CRT expression in P-CSLCs and pancreatic cancer tissues.

**Expression of CRT, CD44v9, and CD47 in pancreatic cancer cells.** Flow cytometry showed that the expression of CRT and CD44v9 on the surface of YPK2-Lm and YPK5-Lm cells was higher than that in the parental cells (Fig. 2a,b). Similarly, CRT surface expression in SW480-Lm cells was elevated compared to parental cells (Fig. S2).

In addition, YPK-Lm cells showed two subsets characterized with $CRT^{high}/CD44v9^{low}$ and $CRT^{low}/CD44v9^{high}$ (Fig. 2c,d).

In contrast, the cytoplasmic expression of CRT was not different between YPK-Lm and YPK parental cells (Fig. 2e,f), suggesting that CRT was transported to the cell surface, which is inconsistent with the mechanism of saturation of Lys-Asp-Glu-Leu (KDEL) motif receptors. The KDEL receptors located on the membrane of the ER and Golgi complex retain CRT in the ER following CRT increase under ER stress.[24]

However, no significant difference in CD47 expression was observed between YPK-Lm and parental cells (Fig. S3a), and no correlation was found between surface expression of CRT and CD47 (Fig. S3b).

It has been shown that the pre-incubation with NAC inhibits CRT translocation to the membrane induced by mitoxantrone, oxaliplatin, and ultraviolet C.[25] To examine whether NAC could decrease CRT expression, we treated YPK-Lm cells with 50 mM NAC for 24 h and found that NAC significantly downregulated the surface expression of CRT ($P = 0.043$), but not of CD44v9, in YPK-Lm cells (Figs. S4,S5).

Transforming growth factor-β has been shown to induce EMT, conferring stem cell properties to cancer cells.[26–28] To investigate whether TGF-β could induce the expression of CD44v9 and CRT, we treated YPK parental cells with 2.5 and 10 ng/mL recombinant human TGF-β1 for 24 h and analyzed for CD44v9 and CRT levels. The results indicated that TGF-β1 did not cause any effect on either CRT or CD44v9 levels in YPK parental cells (Fig. S6).

**ATP-binding cassette transporter activity in YPK-Lm.** The fraction of Hoechst 33342-excreting (SP) cells among YPK2 parental cells was only 0.338% compared to 34.0% in YPK2-Lm cells (Fig. 2g). Similarly, the SP fraction in YPK5-Lm cells was higher (12.9%) than that in YPK5 parental cells (1.72%) (Fig. 2h). In addition, as shown in Figure 3, the SP fraction in $CRT^{high}/CD44v9^{low}$ cells in YPK-Lm cells (Fig. 3b,f) was larger

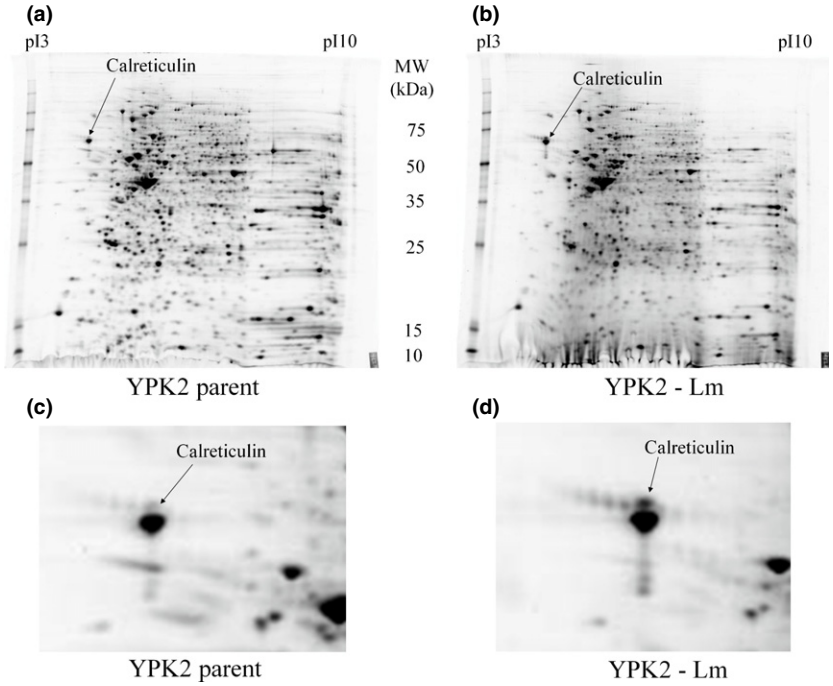


**(e)**

| Start - End | Observed mass | Calculated mass | Score | Sequence |
|---|---|---|---|---|
| 25 – 36 | 1410.65 | 1409.62 | 35 | EQFLDGDGWTSR |
| 143 – 151 | 1147.68 | 1146.65 | 53 | KVHVIFNYK |

```
  1 MLLSVPLLLG LLGLAVAEPA VYFKEQFLDG DGWTSRWIES KHKSDFGKFV
 51 LSSGKFYGDE EKDKGLQTSQ DARFYALSAS FEPFSNKGQT LVVQFTVKHE
101 QNIDCGGGYV KLFPNSLDQT DMHGDSEYNI MFGPDICGPG TKKVHVIFNY
151 KGKNVLINKD IRCKDDEFTH LYTLIVRPDN TYEVKIDNSQ VESGSLEDDW
201 DFLPPKKIKD PDASKPEDWD ERAKIDDPTD SKPEDWDKPE HIPDPDAKKP
251 EDWDEEMDGE WEPPVIQNPE YKGEWKPRQI DNPDYKGTWI HPEIDNPEYS
301 PDPSIYAYDN FGVLGLDLWQ VKSGTIFDNF LITNDEAYAE EFGNETWGVT
351 KAAEKQMKDK QDEEQRLKEE EEDKKRKEEE EAEDKEDDED KDEDEEDEED
401 KEEDEEEDVP GQAKDEL
```

**Fig. 1.** Identification of calreticulin. Representative images of 2-D gel electrophoresis of silver-stained proteins from YPK2 parental cells (a) and YPK2-Lm cells (b). (c) Magnified image of (a). (d) Magnified image of (b). (e) Identification of calreticulin using MALDI TOF/TOF mass spectrometry. Matched peptides are shown in bold red. MW, molecular weight.

than that in $CRT^{low}/CD44v9^{high}$ cells (Fig. 3c,g) or $CRT^{high}/CD44v9^{high}$ cells (Fig. 3d,h).

These results suggest increased drug resistance in P-CSLCs, especially in the $CRT^{high}/CD44v9^{low}$ subpopulation, compared to the rest of the cancer cell population.

**Correlation between CRT and CD44v9 expression and clinical outcome.** In total, 77 patients from Yamaguchi University Hospital and 64 patients from Osaka University Hospital were analyzed; among them, 61 were excluded and 80 were eligible for the study. The process of patient selection is shown in Figure 4. Almost one-third of the patients ($n = 26$) were treated with preoperative chemoradiotherapy, and most of them ($n = 67$) received postoperative adjuvant chemotherapy or immunotherapy.

Representative images of CRT expression in patients' samples are shown in Figure 5. Calreticulin was mainly found in the cytoplasm of normal and cancerous tissues, and had higher expression in the acinus and lower in the islets and ducts of normal pancreatic tissues. Representative images of CD44v9 expression are shown in Figure S7(a). Variant isoform 9 of CD44 was found in the cytoplasm and membrane of normal and cancerous tissues; in normal pancreatic tissues, its expression level was the same in the acinus, islets, and ducts. The intensity of CD44v9 expression in the membrane was scored as strong. The analysis of CRT and CD44v9 staining intensity indicated that there was a significant correlation between IHC scores of CRT and CD44v9 (correlation coefficient, 0.356 [0.148–0.534], $P = 0.0012$).

Cox's regression analysis was used to assess the relationship between clinicopathological features and overall survival. Stepwise backward elimination was used to select significant independent variables. Cox's proportional model included the following variables: previously reported prognostic factors after tumor resection (tumor size, lymph node metastasis,

**Fig. 2.** Flow cytometry analysis of pancreatic cell lines. (a,b) Expression of calreticulin (CRT; left panels) and CD44 variant isoform 9 (CD44v9; right panels) on the surface of (a) YPK2-Lm cells and YPK2 parental cells and (b) YPK5-Lm cells and YPK5 parental cells. (c,d) Expression of CRT and CD44v9 on (c) YPK2 parental cells (left panel) and YPK2-Lm cells (right panel) and on (d) YPK5 parental cells (left panel) and YPK5-Lm cells (right panel). (e,f) Intracellular expression of CRT in (e) YPK2-Lm cells (right panel) and YPK2 parental cells (left panel) and in (f) YPK5-Lm cells (right panels) and YPK5 parental cells (left panels). (g,h) Hoechst 33342 dye exclusion in (g) YPK2 parental cells (left panels) and YPK2-Lm cells (right panels) and in (h) YPK5 parental cells (left panels) and YPK5-Lm cells (right panels). ns, Not significant; RFI, relative fluorescence intensity.

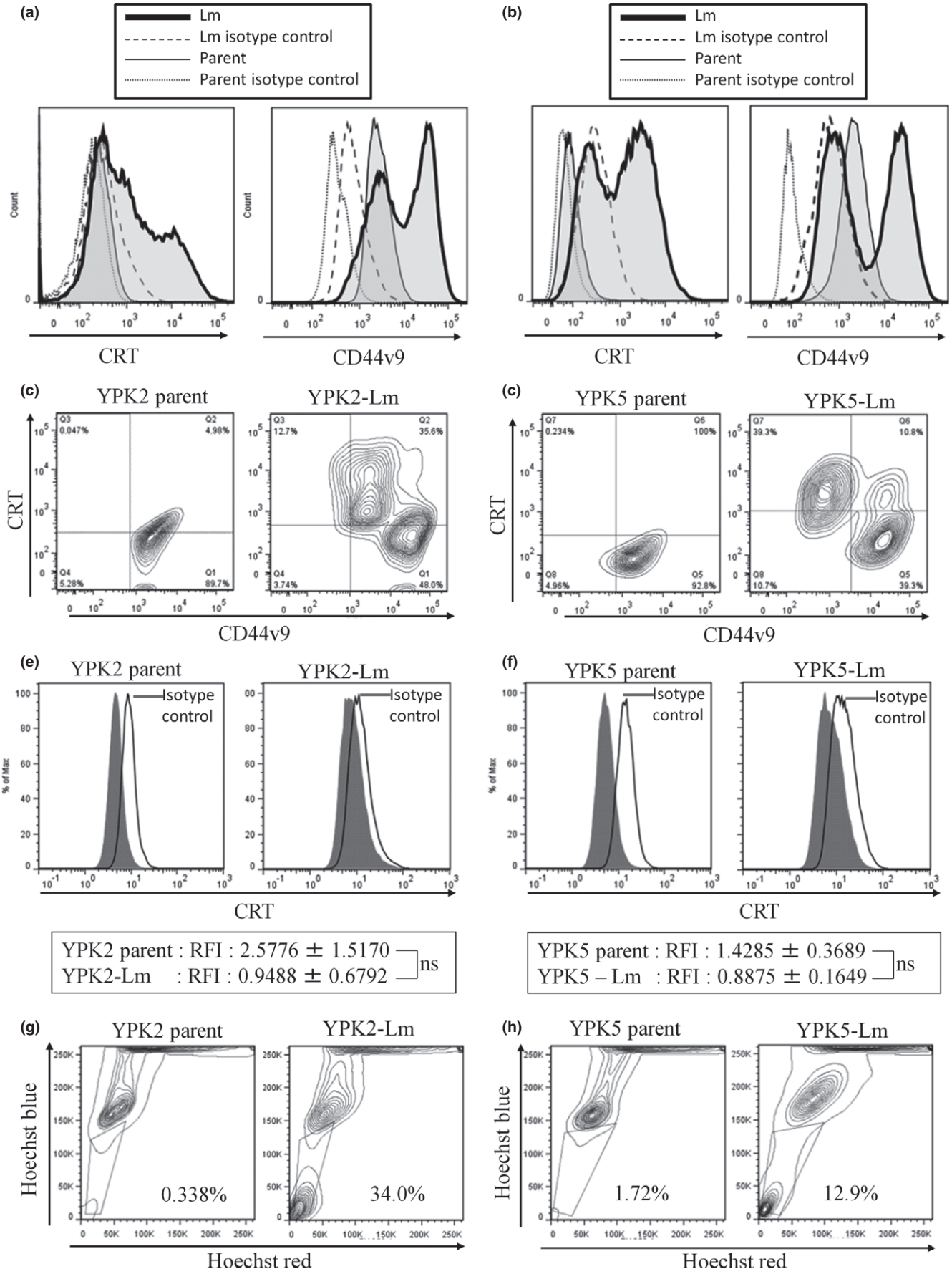

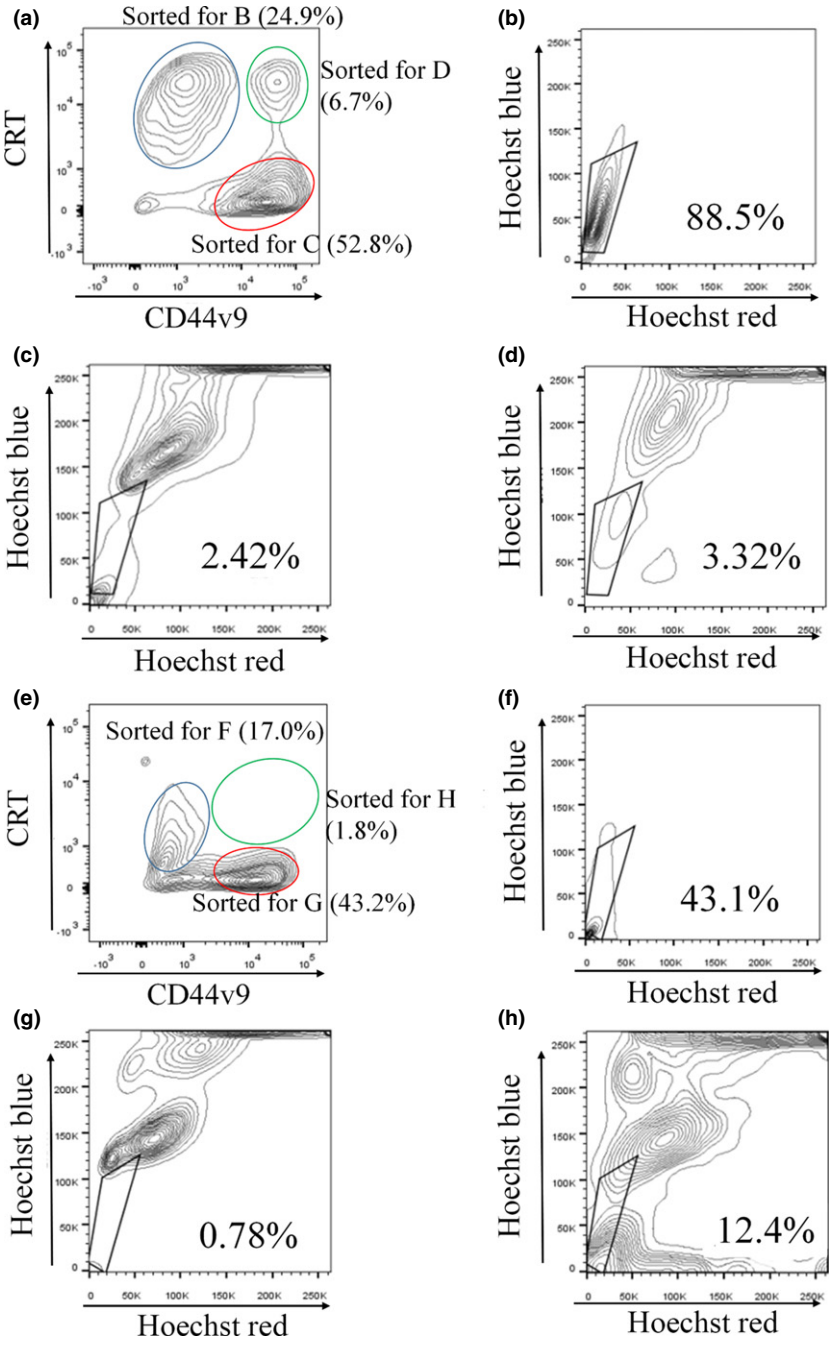


**Fig. 3.** Side population (SP) fraction in sorted cells from YPK-Lm pancreatic cancer cells. (a) Sorted populations in YPK2-Lm. YPK2-Lm cells were sorted into calreticulin (CRT)$^{high}$/CD44 variant isoform 9 (CD44v9)$^{low}$ (blue circle), CRT$^{low}$/CD44v9$^{high}$ (red circle), and CRT$^{high}$/CD44v9$^{high}$ (green circle) subpopulations and ATP-binding cassette transporter activity was analyzed independently. (b) SP fraction in CRT$^{high}$/CD44v9$^{low}$ was 88.5%. (c) SP fraction in CRT$^{low}$/CD44v9$^{high}$ was 2.42%. (d) SP fraction in CRT$^{high}$/CD44v9$^{high}$ was 3.32%. (e) Sorted populations in YPK5-Lm. YPK5-Lm cells were sorted into CRT$^{high}$/CD44v9$^{low}$ (blue circle), CRT$^{low}$/CD44v9$^{high}$ (red circle), and CRT$^{high}$/CD44v9$^{high}$ (green circle) subpopulations and ATP-binding cassette transporter activity was analyzed independently. (f) SP fraction in CRT$^{high}$/CD44v9$^{low}$ was 43.1%. (g) SP fraction in CRT$^{low}$/CD44v9$^{high}$ was 0.78%. (h) SP fraction in CRT$^{high}$/CD44v9$^{high}$ was 12.4%.

perineural invasion, and well-differentiated histology),[29–31] T factor in the TNM staging system, age at surgery, gender, tumor location, portal invasion, IHC scores for CRT and CD44v9, and preoperative and postoperative therapies. In this study, we found that the IHC score for CRT ($P < 0.01$), age ($P < 0.01$), and postoperative chemotherapy or immunotherapy ($P < 0.05$) were independent prognostic factors (Table 1).

Because the median value of the IHC score for CRT was 150 and the best balancing point of sensitivity and specificity for recurrence prediction within a year was 145.27 (sensitivity = specificity = 65.2%), we set 150 as the cut-off level of the IHC score for CRT. The patients were classified according to CRT and CD44v9 expression: high CRT (IHC score ≥150; $n = 43$) and low CRT (IHC score < 150; $n = 37$), and high CD44v9 (IHC score ≥ 165; $n = 40$) and low CD44v9 (IHC score < 165; $n = 40$).

The relationship between clinical features and CRT levels is shown in Table 2. In the high CRT group, there were more cases with an invasion depth greater than T3 ($P = 0.013$), stage II disease ($P = 0.048$), perineural invasion ($P = 0.030$), high CD44v9 expression ($P = 0.004$), and no preoperative chemoradiotherapy ($P = 0.017$). Patients with high CRT expression had poorer recurrence-free survival ($P = 0.0127$) and overall survival ($P = 0.0221$) than those with low CRT expression (Fig. 6). In contrast, CD44v9 level was unrelated to the clinical outcome (Fig. S7b).

Interestingly, there were no differences in CRT scores and CRT expression sites between patients treated or not with preoperative chemoradiotherapy (147.3 ± 54.6 *vs*

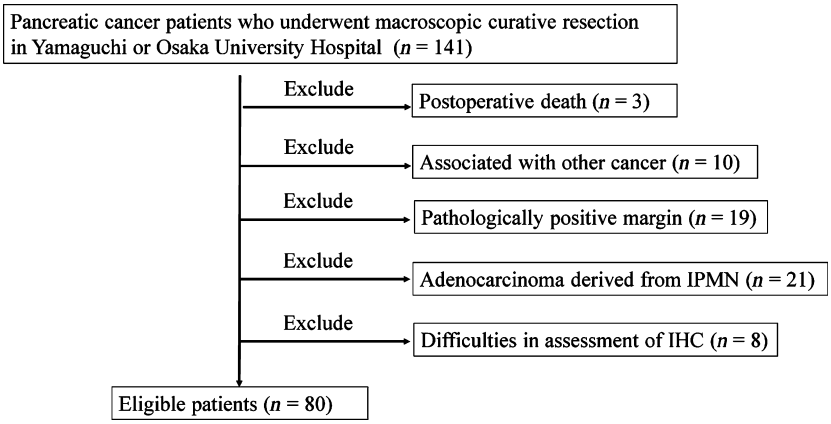


**Fig. 4.** Flow chart of patient selection for this study. IHC, immunohistochemistry; IPMN, intraductal papillary mucinous neoplasm.

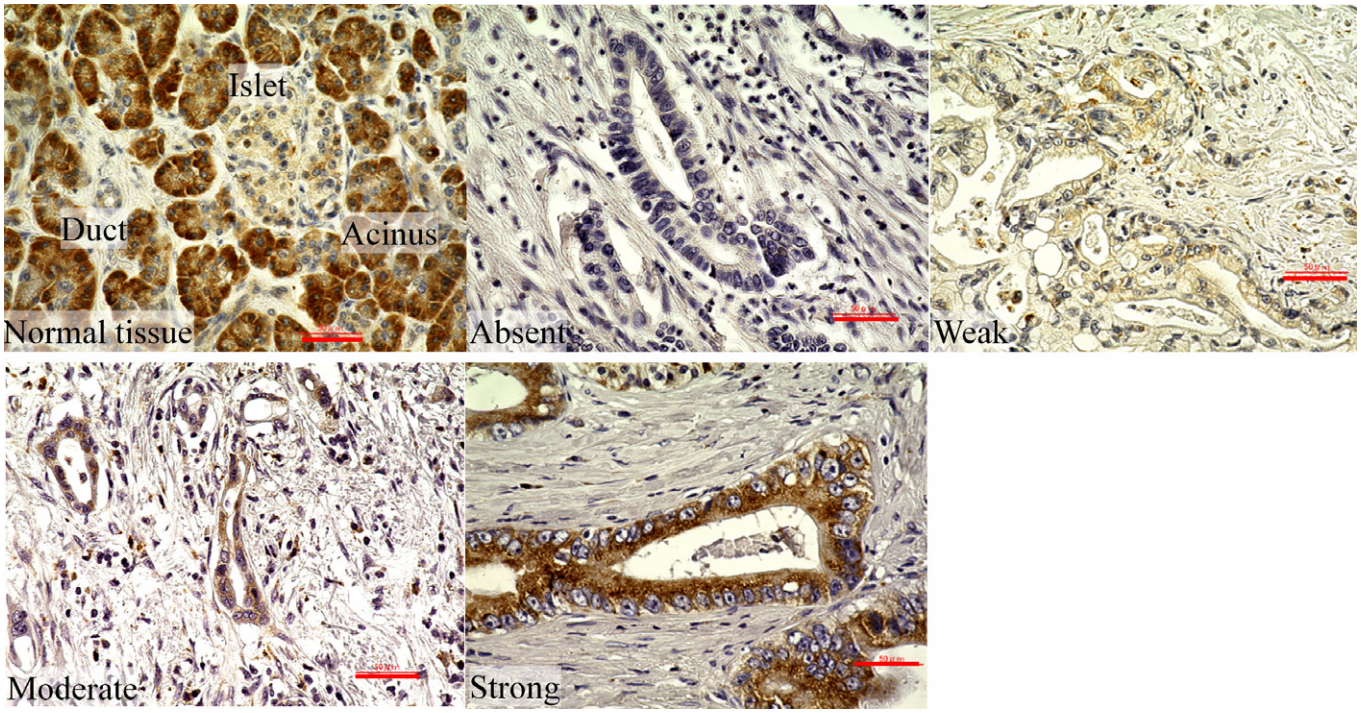


**Fig. 5.** Calreticulin (CRT) expression in resected pancreatic tumor samples. CRT levels were high in the acinus, moderate in the islets, and weak in the ducts of normal pancreatic tissue (left upper panel). In cancerous tissues, CRT expression was categorized as absent (middle upper panel), weak (right upper panel), moderate (left lower panel), and strong (middle lower panel). Scale bar = 50 μm.

174.7 ± 61.8, $P = 0.0575$), although some reports showed that chemotherapy triggered CRT expression.[25] The discrepancy may be attributed to the fact that we undertook preoperative chemoradiotherapy 4–7 weeks prior to surgical resection, and CRT expression might have decreased during this period.

**Colocalization of CRT and CD44v9 expression.** The cases with high levels of both CRT and CD44v9 were examined for intratumor localization of these proteins by immunochemistry. The results indicated that CRT and CD44v9 were partially colocalized in pancreatic cancer tissues (Figs 7,S8).

## Discussion

In the present study, we showed, for the first time, that CRT was highly expressed in P-CSLCs and that its expression in pancreatic cancer tissue was related to patients' survival.

It has been reported that cancer cells acquire stemness properties through EMT[27] and that TGF-β released from cancer cells and their microenvironments promotes EMT and tumor drug resistance.[32,33] However, in this investigation we did not observe TGF-β1 effects on the expression of CRT and CD44v9 in pancreatic cancer cells. In our previous study, we showed that, although the release of TGF-β1 and TGF-β3 by YPK-Lm cells was lower than that by YPK parental cells, mesenchymal markers such as SNAI1 and ZEB2 were highly expressed in YPK-Lm cells.[11] More than half of pancreatic cancer patients were found to carry inactivating mutations of SMAD4, a downstream regulator of TGF-β receptor.[1,34] These findings suggest that YPK-Lm cells acquire stemness through a unique EMT mechanism not requiring TGF-β.

Calreticulin is an ER chaperone that plays important roles in $Ca^{2+}$ homeostasis and quality control of protein folding in normal cells. No definitive reasons for the high CRT expression of

**Table 1. Cox's proportional hazard analysis of overall survival in 80 patients with pancreatic cancer**

| Variable | β | SE | *P*-value | Hazard ratio (95% CI) |
|---|---|---|---|---|
| Age | 0.051 | 0.017 | 0.002 | 1.053 (1.019–1.088) |
| CRT IHC score | 0.007 | 0.002 | 0.004 | 1.007 (1.002–1.011) |
| Postoperative therapy | −0.815 | 0.365 | 0.026 | 0.443 (0.216–0.905) |

CI, confidence interval; CRT, calreticulin; IHC, immunohistochemistry; SE, standard error.

**Table 2. Relationship between calreticulin (CRT) expression and clinical features of pancreatic cancer patients**

| Variable | CRT expression | | *P*-value |
|---|---|---|---|
| | Low (*n* = 37) | High (*n* = 43) | |
| Age, years | | | |
| Mean ± SD | 68.1 ± 7.6 | 65.6 ± 9.5 | 0.199 |
| Gender, *n* | | | |
| Male | 17 | 18 | 0.713 |
| Female | 20 | 25 | |
| Tumor location, *n* | | | |
| pancreatic head | 24 | 31 | 0.487 |
| pancreatic body and tail | 13 | 12 | |
| Tumor size, mm | | | |
| Mean ± SD | 25.7 ± 9.9 | 29.8 ± 17.8 | 0.356 |
| Differentiation, *n* | | | |
| Well | 1 | 5 | 0.139 |
| Moderate–poor | 36 | 38 | |
| Invasion depth, *n* | | | |
| T1 | 5 | 2 | **0.013** |
| T2 | 5 | 0 | |
| T3 | 27 | 41 | |
| Lymph node metastasis, *n* | | | |
| Negative | 21 | 20 | 0.361 |
| Positive | 16 | 23 | |
| TNM stage, *n* | | | |
| I | 7 | 2 | **0.048** |
| II | 30 | 41 | |
| Perineural invasion | | | |
| Negative | 9 | 3 | **0.030** |
| Positive | 28 | 40 | |
| Portal invasion | | | |
| Negative | 24 | 26 | 0.685 |
| Positive | 13 | 17 | |
| Preoperative therapy, *n* | | | |
| None | 20 | 34 | **0.017** |
| Performed | 17 | 9 | |
| Postoperative therapy, *n* | | | |
| None | 5 | 8 | 0.538 |
| Performed | 32 | 35 | |
| CD44v9 expression, *n* | | | |
| Low | 25 | 15 | **0.004** |
| High | 12 | 28 | |

Bold values indicate significance. CD44v9, CD44 variant isoform 9.

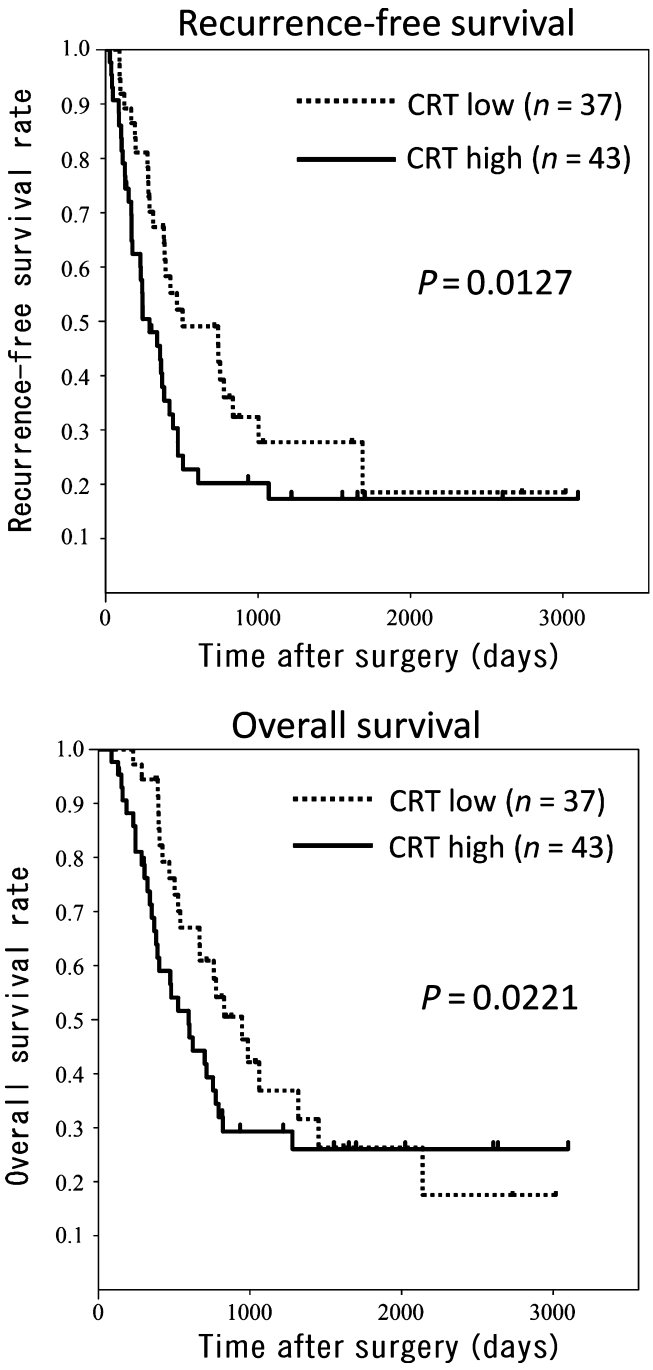


**Fig. 6.** Kaplan–Meier curves of recurrence-free and overall survival rates among pancreatic cancer patients. Solid line, high calreticulin (CRT) expression group (*n* = 43); dotted line, low CRT expression group (*n* = 37).

acinar cells in clinical samples were found in the previous reports, or in our study. Although our focus is more on CRT expressed on the membrane, CRT is mainly located in the ER. Because the ER is a place where protein is synthesized in cells, acinar cells have a large ER to facilitate the synthesis of many proteins;[35] therefore, abundant CRT may exist in normal acinar cells. Stress factors, including chemotherapeutic agents and radiation, promoted the accumulation of misfolded proteins in the ER, activating the "unfolded protein response" such as surface translocation of CRT through the formation of ROS.[25] We found that NAC, a ROS scavenger, could decrease the surface expression of CRT, suggesting that CRT exposure is regulated by ROS and oxidative stress. The antioxidant effect of NAC is unrelated to CD44v9 expression,[10] and other studies reported that intracellular ROS levels in CSCs are low,[36,37] which is contrary to our finding that NAC downregulated CRT, suggesting high intracellular ROS levels in P-CSLCs.

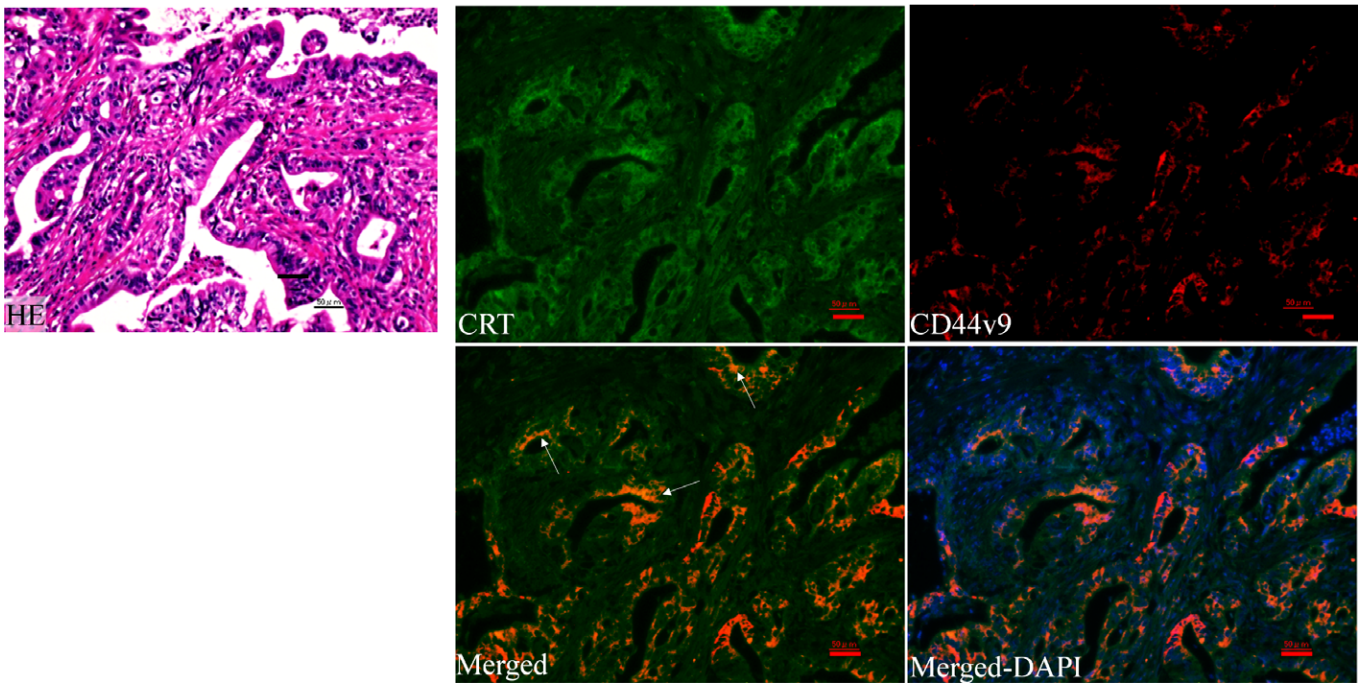


**Fig. 7.** Immunofluorescence staining of CRT (green) and CD44 variant isoform 9 (CD44v9) (red) showing their partial colocalization in pancreatic cancer tissues (left lower panel, merged image, arrows). Nuclei were stained with DAPI (blue). Scale bar = 50 μm.

Although CRT and CD44v9 were colocalized in pancreatic cancer tissues (Figs 5b,S8), flow cytometry analysis suggests that cells with high expression of CRT or CD44v9 represent distinct cell populations. The function of each cell subset is unclear as the findings are controversial. Although the SP phenotype is not a general property of CSLCs,[38] some SP cells are believed to be involved in tumor initiation and drug resistance.[39] Our results show that $CRT^{high}/CD44v9^{low}$ cells expressed the ABC transporter at a higher level than $CRT^{low}/CD44v9^{high}$ cells, suggesting that CRT is a more sensitive surface marker of SP cells or P-CSLCs than CD44v9.

Our results are not in agreement with previous data showing that CRT surface expression did not differ between cancer cells and CSCs in bladder tumors and glioblastoma,[19] which may be attributed to the difference in cancer types. Furthermore, Chao *et al.*[19] have shown that cells with CRT surface expression have tumorigenic potential similar to those without CRT expression, indicating that CRT is expressed not only on apoptotic cells but also on viable cells.

There are two major discrepancies in CRT and CD44v9 expression between cell lines and clinical samples. First, we showed that expression of CRT on the cell surface, not in the cytoplasm, is an important feature of P-CSLCs. Second, $CRT^{high}/CD44v9^{low}$, $CRT^{low}/CD44v9^{high,}$ and $CRT^{high}/CD44v9^{high}$ populations are clearly distinguished populations *in vitro*. However, we could not obtain these two findings in clinical samples. In clinical samples, most of the stained cells were cancer cells. It was difficult to distinguish membranous expression of CRT from cytoplasmic expression in IHC. Thus our observations *in vivo* included cytoplasmic expression of CRT in cancer cells, which might have given rise to the discrepancy between the *in vitro* and *in vivo* results. The data described above and those regarding the ABC transporter suggest that CRT and CD44v9 are independent surface markers for P-CSLCs.

Although surface CRT acts as an "eat-me" signal facilitating innate immunity,[13] it has also been shown that CRT overexpression is associated with poor survival of patients with esophageal cancer,[40] gastric cancer,[41] and pancreatic cancer,[16] which is consistent with our results. There are two possible explanations for this discrepancy.[19] First, cancer cells expressing surface CRT may resist phagocytosis by coexpressing CD47 as an antiphagocytic signal. Although our results did not show a linear relationship between CRT and CD47 expression, which conflicts with previous findings, CD47 levels in YPK-Lm cells were similar to those in YPK parental cells. Therefore, the role of CD47 expression in conferring immune privilege to P-CSLCs is unclear. Second, CRT surface expression could contribute to an aggressive phenotype of cancer cells not associated with their resistance to phagocytosis. In this regard, it has been reported that CRT promotes cancer cell migration and invasion by upregulating neuropilin-1, MMP2, MMP9, and focal adhesion kinase,[42] as well as cell motility and resistance to anoikis by activating the phosphoinositide 3-kinase/protein kinase B pathway.[43] Although CRT is related to several CSC properties, the role of CRT in the functional activity of CSCs has not been elucidated. Calreticulin present on the surface of cancer cells is recognized by LDL receptor-related protein 1/CD91 on macrophages, activating phagocytosis of cancer cells.[44] However, the polarization toward the M2 profile in tumor-associated macrophages[45] could inhibit adequate recognition of CRT in the tumor microenvironment. Thus, the enhancement of macrophage recognition of CRT on P-CSLCs by stimulating M1 polarization of tumor-associated macrophages in the tumor microenvironment could be a novel therapeutic approach to induce immune responses against P-CSLCs.

At present, it is not known whether the role of CRT surface expression in CSLCs is extended beyond the ER stress. However, CRT can be one of the few candidate therapeutic targets in cancer because its expression on CSLC surface may present an exceptional mechanism used by cancer cells to evade immune surveillance.[46]

Regarding the clinical application of targeting CRT expression in P-CSLCs, immunotherapy may be the most promising. Immunotherapy combined with chemotherapy can be used to induce CRT expression on the surface of tumor cells. However, chemotherapy represents here a double-edged sword because it can induce CRT exposure while inhibiting antitumor T-cell response through myelosuppression. Therefore, immunogenic phagocytosis[47] of P-CSLCs could be induced without preceding chemotherapy, so that CRT is intrinsically expressed on P-CSLCs. There is a large difference in CRT expression level between normal cells (low or none except for acinus cells in the pancreas) and P-CSLCs (very high). This difference is useful for immunological targeting and avoiding adverse effects. It is possible that immunotherapy targeting CRT inappropriately recognizes normal tissues expressing CRT at a much lower level. However, the level of recognition in such cases is not high, and the adverse effects of immunotherapies are low.

In conclusion, we have shown that CRT is highly expressed in P-CSLCs, which is related to poorer survival of pancreatic cancer patients after radical resection. Further investigations on CRT expression on CSLCs will lead to the development of novel therapeutic targets to prevent the progression of pancreatic cancer.

## Acknowledgments

This study was supported by the Translational Research Promotion Grant from Yamaguchi University Hospital (to K.Y.) We would like to thank Ms. Akiko Sano, Ms. Kaori Kaneyasu, and Ms. Hiroko Takenouchi for technical assistance. We also would like to thank Editage and Manami Kobayashi for assistance with English language editing.

## Disclosure Statement

Kiyoshi Yoshimura owns stock in Noile-Immune Biotech, Inc. and received research funds from Noile-Immune Biotech, Inc. Shigefumi Yoshino received honoraria as a lecture fee from MSD corporation, outside the submitted work. Shoichi Hazama received research funds from NEC Corporation and Toyo Kohan Corporation. The other authors have no conflicts of interest to declare.

## Abbreviations

| | |
|---|---|
| ABC | ATP-binding cassette |
| CD44v | variant isoform of CD44 |
| CRT | calreticulin |
| CSC | cancer stem cell |
| CSLC | cancer stem-like cell |
| EMT | epithelial–mesenchymal transition |
| ER | endoplasmic reticulum |
| IHC | immunohistochemistry |
| MS/MS | tandem mass spectrometry |
| NAC | N-acetyl-L-cysteine |
| TGF | transforming growth factor |
| P-CSLC | pancreatic cancer stem-like cell |
| ROS | reactive oxygen species |
| SP | side population |

## References

1 Ryan DP, Hong TS, Bardeesy N. Pancreatic adenocarcinoma. *N Engl J Med* 2014; **371**: 1039–49.
2 Clevers H. The cancer stem cell: premises, promises and challenges. *Nat Med* 2011; **17**: 313–9.
3 Li X, Lewis MT, Huang J *et al.* Intrinsic resistance of tumorigenic breast cancer cells to chemotherapy. *J Natl Cancer Inst* 2008; **100**: 672–9.
4 Zhou BB, Zhang H, Damelin M, Geles KG, Grindley JC, Dirks PB. Tumour-initiating cells: challenges and opportunities for anticancer drug discovery. *Nat Rev Drug Discov* 2009; **8**: 806–23.
5 Li C, Heidt DG, Dalerba P *et al.* Identification of pancreatic cancer stem cells. *Cancer Res* 2007; **67**: 1030–7.
6 Hermann PC, Herrler T, Aicher A *et al.* Distinct populations of cancer stem cells determine tumor growth and metastatic activity in human pancreatic cancer. *Cell Stem Cell* 2007; **1**: 313–23.
7 Rasheed ZA, Yang J, Wang Q *et al.* Prognostic significance of tumorigenic cells with mesenchymal features in pancreatic adenocarcinoma. *J Natl Cancer Inst* 2010; **102**: 340–51.
8 Li C, Hynes M, Dosch J *et al.* c-Met is a marker of pancreatic cancer stem cells and therapeutic target. *Gastroenterology* 2011; **141**: 2218–27.
9 Sureban SM, May R, Qu D *et al.* DCLK1 regulates pluripotency and angiogenic factors via microRNA-dependent mechanisms in pancreatic cancer. *PLoS ONE* 2013; **8**: e73940.
10 Ishimoto T, Nagano O, Yae T *et al.* CD44 variant regulates redox status in cancer cells by stabilizing the xCT subunit of system xc(-) and thereby promotes tumor growth. *Cancer Cell* 2011; **19**: 387–400.
11 Watanabe Y, Yoshimura K, Yoshikawa K *et al.* A stem cell medium containing neural stimulating factor induces a pancreatic cancer stem-like cell-enriched population. *Int J Oncol* 2014; **45**: 1857–1866.
12 Yoshida GJ, Saya H. Therapeutic strategies targeting cancer stem cells. *Cancer Sci* 2016; **107**: 5–11.
13 Obeid M, Tesniere A, Ghiringhelli F *et al.* Calreticulin exposure dictates the immunogenicity of cancer cell death. *Nat Med* 2007; **13**: 54–61.
14 Yamamura Y, Tsuchikawa T, Miyauchi K *et al.* The key role of calreticulin in immunomodulation induced by chemotherapeutic agents. *Int J Clin Oncol* 2015; **20**: 386–94.
15 Hong SH, Misek DE, Wang H *et al.* An autoantibody-mediated immune response to calreticulin isoforms in pancreatic cancer. *Cancer Res* 2004; **64**: 5504–10.
16 Sheng W, Chen C, Dong M *et al.* Overexpression of calreticulin contributes to the development and progression of pancreatic cancer. *J Cell Physiol* 2014; **229**: 887–97.
17 Yamamoto K, Yahara N, Gondo T, Ishihara T, Oka M. Establishment and characterization of a new human pancreatic cancer cell line, YPK-1. *Bull Yamaguchi Med Sch* 2002; **49**: 33–42.
18 Gerashchenko BI, Yamagata A, Oofusa K, Yoshizato K, de Toledo SM, Howell RW. Proteome analysis of proliferative response of bystander cells adjacent to cells exposed to ionizing radiation. *Proteomics* 2007; **7**: 2000–8.
19 Chao MP, Jaiswal S, Weissman-Tsukamoto R *et al.* Calreticulin is the dominant pro-phagocytic signal on multiple human cancers and is counterbalanced by CD47. *Sci Transl Med* 2010; **22**: 63–84.
20 Zhou J, Wang CY, Liu T *et al.* Persistence of side population cells with high drug efflux capacity in pancreatic cancer. *World J Gastroenterol* 2008; **14**: 925–30.
21 Goodell MA, Brose K, Paradis G, Conner AS, Mulligan RC. Isolation and functional properties of murine hematopoietic stem cells that are replicating in vivo. *J Exp Med* 1996; **183**: 1797–806.
22 Japan Pancreas Society. *General Rules for the Study of Pancreatic Cancer, The 6th Edition*, Revised Version edn. Tokyo, Japan: Kanehara, 2013.
23 Lee HJ, Xu X, Choe G *et al.* Protein overexpression and gene amplification of epidermal growth factor receptor in nonsmall cell lung carcinomas: Comparison of four commercially available antibodies by immunohistochemistry and fluorescence in situ hybridization study. *Lung Cancer* 2010; **68**: 375–82.
24 Wiersma VR, Michalak M, Abdullah TM, Bremer E, Eggleton P. Mechanisms of translocation of ER Chaperones to the cell surface and immunomodulatory roles in cancer and autoimmunity. *Front Oncol* 2015; **5**: doi: 10.3389/fonc.2015.00007.
25 Panaretakis T, Kepp O, Brockmeier U *et al.* Mechanisms of pre-apoptotic calreticulin exposure in immunogenic cell death. *EMBO J* 2009; **28**: 578–90.
26 Han D, Wu G, Chang C *et al.* Disulfiram inhibits TGF-beta-induced epithelial-mesenchymal transition and stem-like features in breast cancer via ERK/NF-κB/Snail pathway. *Oncotarget* 2015; **16**: 40907–19.
27 Mani SA, Guo W, Liao MJ *et al.* The epithelial-mesenchymal transition generates cells with properties of stem cells. *Cell* 2008; **133**: 704–15.
28 Oshimori N, Oristian D, Fuchs E. TGF-beta promotes heterogeneity and drug resistance in squamous cell carcinoma. *Cell* 2015; **160**: 963–76.
29 Chatterjee D, Katz MH, Rashid A *et al.* Perineural and intraneural invasion in posttherapy pancreaticoduodenectomy specimens predicts poor prognosis

in patients with pancreatic ductal adenocarcinoma. *Am J Surg Pathol* 2012; **36**: 409–17.
30 Lim JE, Chien MW, Earle CC. Prognostic factors following curative resection for pancreatic adenocarcinoma: a population-based, linked database analysis of 396 patients. *Ann Surg* 2003; **237**: 74–85.
31 Richter A, Niedergethmann M, Sturm JW, Lorenz D, Post S, Trede M. Long-term results of partial pancreaticoduodenectomy for ductal adenocarcinoma of the pancreatic head: 25-year experience. *World J Surg* 2003; **27**: 324–9.
32 Labelle M, Begum S, Hynes RO. Direct signaling between platelets and cancer cells induces an epithelial-mesenchymal-like transition and promotes metastasis. *Cancer Cell* 2011; **20**: 576–90.
33 Massague J. TGFbeta signalling in context. *Nat Rev Mol Cell Biol* 2012; **13**: 616–30.
34 Massague J. TGFbeta in Cancer. *Cell* 2008; **134**: 215–30.
35 Ye R, Mareninova OA, Barron E *et al.* Grp78 heterozygosity regulates chaperone balance in exocrine pancreas with differential response to cerulein-induced acute pancreatitis. *Am J Pathol* 2010; **177**: 2827–36.
36 Diehn M, Cho RW, Lobo NA *et al.* Association of reactive oxygen species levels and radioresistance in cancer stem cells. *Nature* 2009; **458**: 780–3.
37 Suzuki S, Okada M, Shibuya K *et al.* JNK suppression of chemotherapeutic agents-induced ROS confers chemoresistance on pancreatic cancer stem cells. *Oncotarget* 2015; **6**: 458–70.
38 Clarke MF, Dick JE, Dirks PB *et al.* Cancer stem cells–perspectives on current status and future directions: AACR Workshop on cancer stem cells. *Cancer Res* 2006; **66**: 9339–44.
39 Li D, Su D, Xue L, Liu Y, Pang W. Establishment of pancreatic cancer stem cells by flow cytometry and their biological characteristics. *Int J Clin Exp Pathol* 2015; **8**: 11218–23.
40 Du XL, Lin DE, Xia SH *et al.* Proteomic profiling of proteins dysregulted in Chinese esophageal squamous cell carcinoma. *J Mol Med* 2007; **85**: 863–75.
41 Chen CN, Chang CC, Su TE *et al.* Identification of calreticulin as a prognosis marker and angiogenic regulator in human gastric cancer. *Ann Surg Oncol* 2009; **16**: 525–33.
42 Shi F, Shang L, Pan BQ *et al.* Calreticulin promotes migration and invasion of esophageal cancer cells by upregulating neuropilin-1 expression via STAT5A. *Clin Cancer Res* 2014; **20**: 6153–62.
43 Du XL, Yang H, Liu SG *et al.* Calreticulin promotes cell motility and enhances resistance to anoikis through STAT3-CTTN-Akt pathway in esophageal squamous cell carcinoma. *Oncogene* 2009; **28**: 3714–22.
44 Gardai SJ, McPhillips KA, Frasch SC *et al.* Cell-surface calreticulin initiates clearance of viable or apoptotic cells through trans-activation of LRP on the phagocyte. *Cell* 2005; **123**: 321–34.
45 Solinas G, Germano G, Mantovani A, Allavena P. Tumor-associated macrophages (TAM) as major players of the cancer-related inflammation. *J Leukoc Biol* 2009; **86**: 1065–73.
46 Bruttel VS, Wischhusen J. Cancer stem cell immunology: key to understanding tumorigenesis and tumor immune escape? *Front Immunol* 2014; **29**: 360.
47 Jinushi M, Yagita H, Yoshiyama H, Tahara H. Putting the brakes on anticancer therapies: suppression of innate immune pathways by tumor-associated myeloid cells. *Trends Mol Med* 2013; **19**: 536–45.

## Supporting Information

Additional Supporting Information may be found online in the supporting information tab for this article:

**Fig. S1.** Flow chart of the study.

**Fig. S2.** Flow cytometry analysis of calreticulin (CRT) expression in SW480 cells.

**Fig. S3.** Calreticulin (CRT) and CD47 expression in YPK parental cells and YPK-Lm cells.

**Fig. S4.** Flow cytometry analysis of calreticulin (CRT) surface expression in N-acetyl-L-cysteine (NAC)-treated YPK2-Lm cells.

**Fig. S5.** Flow cytometry analysis of CD44 variant isoform 9 (CD44v9) surface expression in N-acetyl-L-cysteine (NAC)-treated YPK2-Lm cells.

**Fig. S6.** Flow cytometry analysis of YPK2 and YPK5 cells incubated with TGF-β1 for 24 h.

**Fig. S7.** Representative images of CD44 variant isoform 9 (CD44v9) expression in pancreatic tissues.

**Fig. S8.** Colocalization of calreticulin (CRT) and CD44 variant isoform 9 (CD44v9) expression in pancreatic cancer tissues analyzed by immunofluorescence.

**Data S1.** Supplementary materials and methods.